HIGH SALINITY RECORDED BY BEDROCK SULFATE ENRICHMENTS AT GALE CRATER. W. Rapin[1], B. L. Ehlmann[1,2], G. Dromart[3], J. Schieber[4], N. Thomas[1], W.W. Fischer[1], V. Fox[1], N. Stein[1], M. Nachon[5], B. Clark[6], L. Kah[7], L. Thompson[8], H. A. Meyer[1], T.S.J. Gabriel[9], C. Hardgrove[9], N. Mangold[10], R.C. Wiens[11], A. Vasavada[2]. [1]Caltech-GPS, wrapin@caltech.edu; [2]Caltech-JPL; [3]Univ. Lyon, LGLTPE, France; [4]Indiana University, Bloomington; [5]Texas A&M University, ; [6]Space Science Institute; [7]Univ. Tennessee-Knoxville; [8]Univ. New Brunswick; [9]Arizona State Univ. (School of Earth and Space Exploration; [10]LPG, Nantes, France; [11]LANL;

Introduction: Sulfate salts deposited in sedimentary basins are geochemical markers of specific climate, source rock, and dissolved gases and ions [1]. On Mars, a diversity of salts is identified and prominent thick layered sulfate deposits are observed at a number of late Noachian to late Hesperian locations (~3.5 Ga) [2]. Their apparent absence in older strata has led to the hypothesis that they represent the diminishing availability of liquid water on Mars [3]. Gale crater provides an exemplary sedimentary succession with clay minerals transitioning to sulfates over ~300 m of stratigraphy [4,5]. Understanding the reason for this transition is one of the primary objectives of the MSL/Curiosity rover investigation. So far, the rover has explored clay-bearing fluviolacustrine sedimentary record in the lowermost stratigraphy [6], and sulfates have been observed, as gypsum crystal pseudomorphs in a thin (~4 m) localized mudstone section [7], but mostly in the form of late diagenetic Ca-sulfate fracture-fills [8,9], and also occasionally as Mg-sulfates associated with sparse diagenetic features such as concretions and dendrites [10,11]. Here we report on bulk enrichments in Ca-sulfates (to 30-50 wt%), hydrated Mg-sulfates (to 33 wt%) within cm-thick planar bedrock exposures (Figures 1 and 2), as well as chlorides [12], observed intermittently over a ~150 m elevation interval of heterolithic facies in the Murray formation. While a prior report on Mg-sulfate proposed a qualitative approach on the presence of sulfur from ChemCam data [13], in this new study we track the presence of sulfur in all enrichments and estimate the content of sulfate-salt observed using an updated calibration of the sulfur signal. We find that the presence of laterally extensive layers enriched in sulfate, occurring intermittently along most of the upper Murray formation, likely has strong implications on depositional and diagenetic environment of these sediments.

Methods and observations: The Ca-sulfate enriched bedrock was analyzed by both the Alpha Particle X-ray Spectrometer (APXS) and ChemCam (providing Laser Induced Breakdown Spectroscopy (LIBS)) instruments. Yet ChemCam sampled a greater variety of bedrock, and observation of point-to-point homogeneous enrichments with its submillimeter footprint indicates that the salt is finely disseminated in the rock at a scale

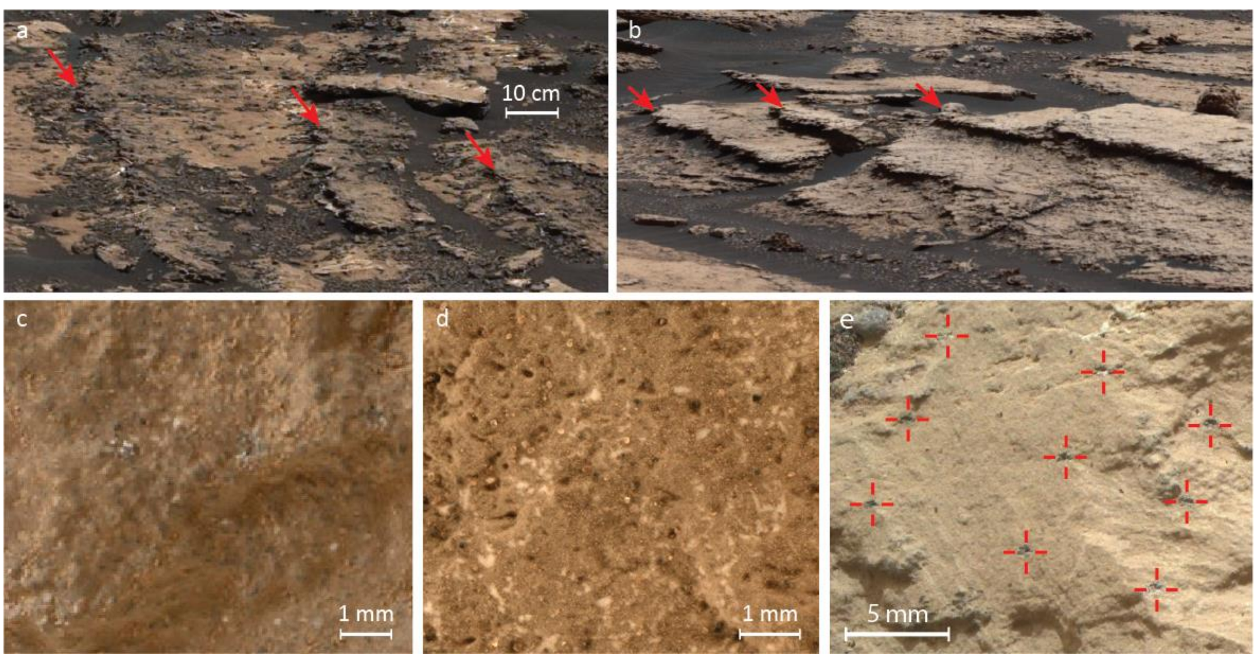

Figure 1: Images of the sulfate enriched lithologies observed in the upper Murray formation: a) Mg-sulfate enriched cm-thick dark-toned layers (red arrow), sol 1680 (ML_mcam08715). b) erosion resistant layers where desseminated Ca-sulfate enrichments have been found, whereas interbedded recessive bedrock has typical Murray composition (CaO <2.5 wt%), sol 1672 (ML_mcam08669). Close-up images of Ca-sulfate enriched bedrocks for c) sandstone with white grains, d) mudstone with elongated euhedral crystals and corresponding hollow molds and e) mudstone with massive or nodular texture but no veins.

similar to sediment grain size. Major elements are quantified from the spectra using a multivariate calibration process [14]. Other elements, like trace [15] and hydrogen [16,17] can be measured simultaneously. For sulfur, a dedicated model is used to quantify. The signal is clearly expressed in the emission spectra by 3 peaks at 543 nm, 545 nm, and 564 nm with significant S enrichments leading to a ~0.2 nm shift in the location of peak centroids at 543 nm and 545 nm, combined with an increase in the magnitude of the 564-nm peak emission, as also observed in laboratory experiments [18]. Targets enriched in Ca-sulfate were carefully selected based on high-resolution (<0.5 mm/pixel) Remote Micro Images (RMI), and larger scale context from MastCam images to rule out contribution from fracture-fill Ca-sulfate veins. Hydrated Mg-sulfate enrichments were also observed by the ChemCam instrument in a specific stratigraphic interval [13] (Figure 2), but were not sampled by the APXS instrument. DAN thermal neutron count rates are consistent with enhanced subsurface hydrogen in the same strata.

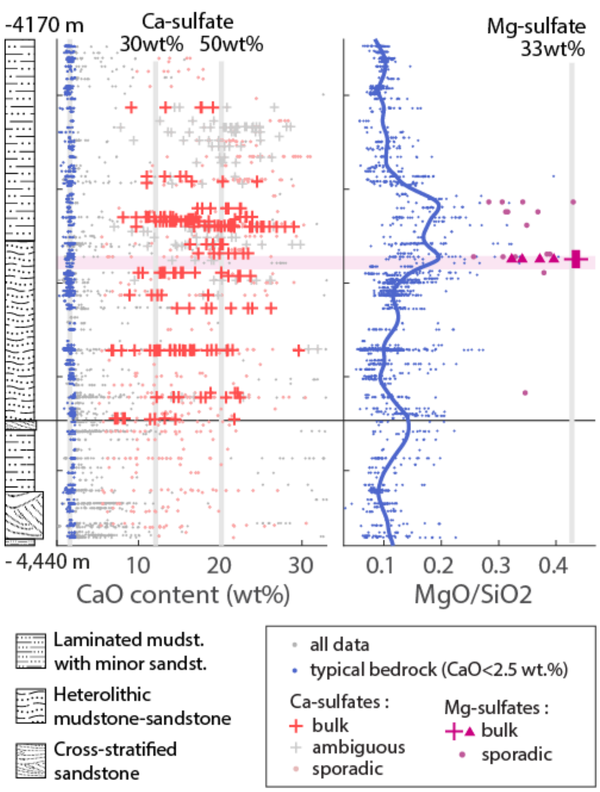

Figure 2: CaO content and MgO/SiO2 as a function of elevation for most of the upper Murray formation members [19].

Discussion: The timing of formation for the sulfate enrichments is crucial to its environmental implications. Since the sulfates are disseminated homogeneously within cm-thick planar bedrock exposures which are not associated to fracture-fill veins, related late stage diagenetic formation seems unlikely. On the other hand, depositional textures of primary salts, such as beds with bottom-growth or cumulate crystals, are not observed. We suggest that early diagenetic precipitation from sulfate brines followed by alteration of textures during diagenesis best explain the observations. Other mineralogical and sedimentary evidence support shrinking of the lake and arid conditions occurred episodically during the deposition of the upper Murray formation [20–22]. A series of smaller lakes with distributive channels could represent a depositional environment consistent with the heterolithic mudstone-sandstones facies observed [19], which coincides with the occurrence of sulfate enrichments (Figure 2). Early deposition of the observed salts in this context could have occurred during subaqueous infiltrations or in the capillary fringe within or in the margin of saline ponds (Figure 3).

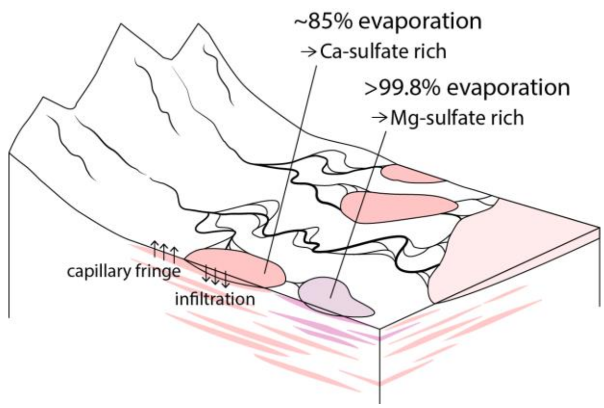

Figure 3: Deposition scenario of the sulfate salts in the margin of the Gale lake basin, possibly forming evaporative ponds fed by distributive channel systems. Percent evaporation corresponds to Ca-sulfate and Mg-sulfate saturation of fluid derived from basalt weathering after Tosca et al. 2005 [23].

References: [1] Eugster H. P. and Hardie L. A. (1978) in: Lerman, A. (Ed.), *Lakes: Chemistry, Geology, Physics*, pp. 237–293. [2] Ehlmann B. L. and Edwards C. S. (2014) *Annu. Rev. Earth Planet. Sci.* 42, 291–315. [3] Bibring J.-P. et al. (2006) *Science* 312, 400–404. [4] Fraeman A. A. et al. (2016) *J. Geophys. Res. Planets* 121, 1713–1736. [5] Milliken R. E. et al. (2010) *Geophys. Res. Lett.* 37. [6] Grotzinger J. P. et al. (2015) *Science* 350. [7] Kah L. C. et al. (2018) *Terra Nova* 30, 431–439. [8] Nachon M. et al. (2014) *J. Geophys. Res. Planets* 119, 2013JE004588. [9] Rapin W. et al. (2016) *Earth Planet. Sci. Lett.* 452, 197–205. [10] Nachon M. et al. (2017) *Icarus* 281, 121–136. [11] VanBommel S. J. et al. (2016) *X-Ray Spectrom.* 45, 155–161. [12] Thomas N. H. et al. (2018) LPSC49 2876. [13] Rapin W. et al. (2018) LPSC49 2936. [14] Clegg S. M. et al. (2017) *Spectrochim. Acta Part B At. Spectrosc.* 129, 64–85. [15] Payré V. et al. (2017) *J. Geophys. Res. Planets* 122, 650–679. [16] Rapin W. et al. (2017) *Spectrochim. Acta Part B At. Spectrosc.* 130, 82–100. [17] Rapin W. et al. (2017) *Spectrochim. Acta Part B At. Spectrosc.* 137, 13–22. [18] Anderson D. E. et al. (2017) *J. Geophys. Res. Planets* 122, 744–770. [19] Bristow T. F. et al. (2018) *Sci. Adv.* 4, eaar3330. [20] Stein N. et al. (2018) *Geology* 46, 515–518. [21] Schieber J. et al. (2017) LPSC48 2311. [22] Fedo C. et al. (2018) LPSC48 2078. [23] Tosca N. J. et al. (2005) *Earth Planet. Sci. Lett.* 240, 122–148.